Visualizing the Outflow Pathway

Future advances in OCT may make it possible to evaluate the functionality of the collector system.

BY LARRY KAGEMANN, PHD, AND JOEL S. SCHUMAN, MD

Parallel advances in optical coherence tomography (OCT) imaging hardware and the sophistication of applied computer vision techniques to OCT imagery have expanded the modality's application in ophthalmology. Since its early use for the assessment of the retinal nerve fiber layer, OCT has been a means of quantifying the structural changes associated with age-related macular degeneration, diabetic retinopathy, and retinitis pigmentosa.[1-6]

Having demonstrated OCT's ability to visualize the lamina cribrosa (LC),[7] we recently published a technique for automated segmentation of the LC (Figure 1).[8-10] As opposed to evaluating the complex anatomy of the limbus, LC analysis is relatively straightforward. On OCT, LC tissue presents as either pores, which actually contain nerve fiber bundles with poor reflectance due to their orientation, or as collagen beams. Defining the border between the two remains nuanced, however, and much work still needs to be done before implementation in clinical devices.

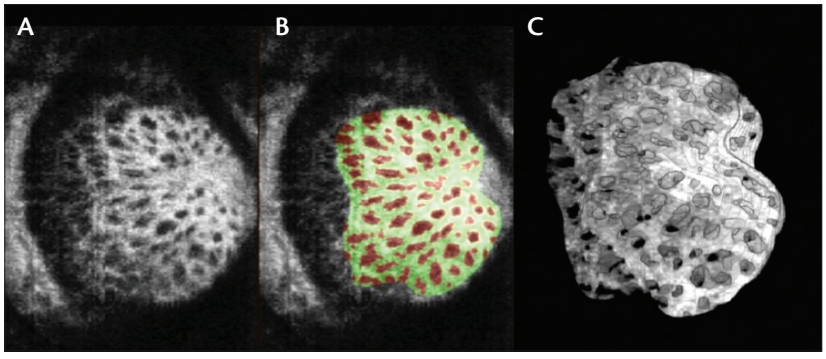

Figure 1. Tissues within the LC (A) appear as either collagen beam (light) or pores (dark), facilitating automated segmentation (B) and allowing three-dimensional (3-D) visualization of the collagen structure (C).

"Unlike cadaveric tissue, in which a minimal number of outflow pathways were open, the living eye has a greater density of patent aqueous vessels."

CHALLENGES

Segmentation of the outflow pathway within the limbus presents a complex challenge. Pilot work in a donor eye perfusion model (Bioptigen OCT [Bioptigen], 200-nm bandwidth light source [SuperLum], 10-second image acquisition time) allowed visualization of the primary aqueous humor outflow pathway.[11] Only outflow pathways were open; other structures within the cadaveric tissue had collapsed. The outflow pathways presented as hyporeflective regions on OCT scans, because mock aqueous solution provided little or no signal. In these tissues, automated segmentation was similar to that in the LC; specifically, image content represented either reflective tissues surrounding the outflow system or the hyporeflective openings of the outflow system itself (Figure 2).

Unlike cadaveric tissue, in which a minimal number of outflow pathways were open (Figure 2), the living eye has a greater density of patent aqueous vessels (Figures 3 and 4). Living tissue presents with both

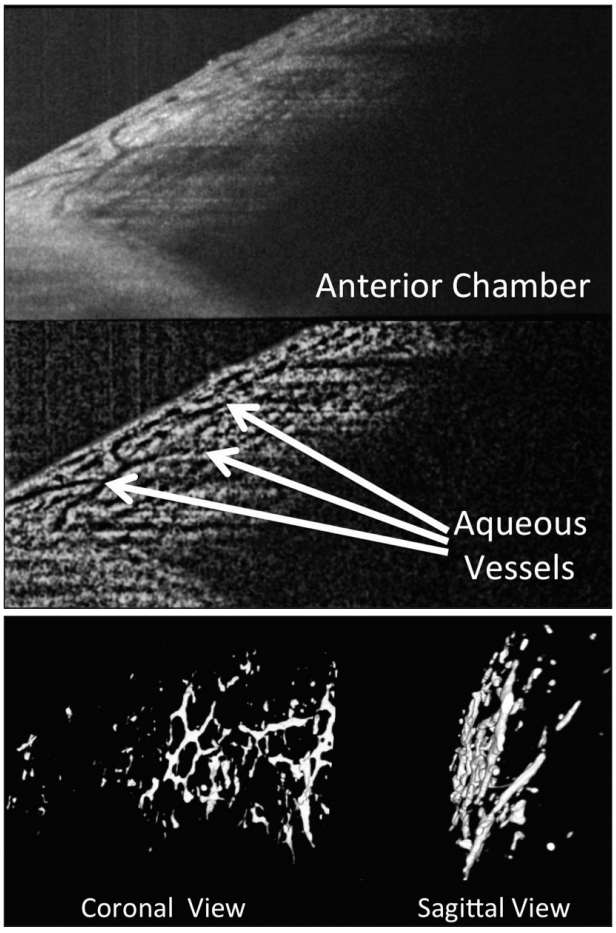

Figure 2. Visualization of open aqueous outflow pathway structures in the limbus of a donor eye in a perfusion model. An OCT scan (top) may be enhanced (center, aqueous pathways shown by arrows). The few pathways opened by outflow in a donor eye may be observed in 3-D (bottom).

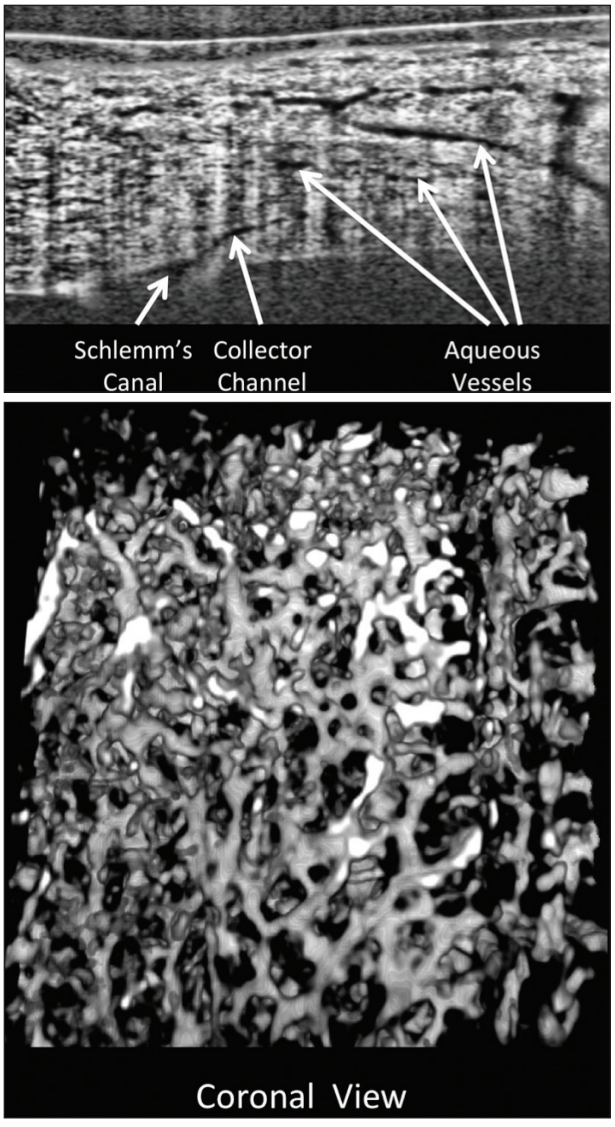

Figure 3. In a living eye, far more aqueous pathways are open, observable from Schlemm canal through the numerous aqueous vessels (top); 3-D visualization shows a dense and overlapping outflow vasculature (bottom).

active blood and aqueous vessels. Moreover, not all visible pathways within the limbus are necessarily collector channels or aqueous veins (Figure 3). Imposing a connectivity criterion on the segmentation would seem to be a viable way to isolate the aqueous pathway, but shadows cast by superficial blood vessels provide dark vertical artifacts within the images, creating false connections between various internal pathways (Figure 3).

Higher-density scanning patterns available on experimental systems improve the visualization of outflow structures, but obscuration by noise and other vessels reduces the clinical utility of the best imaging of the outflow systems currently available. Noise suppression techniques improve the visualization of outflow structure but at a cost. Specifically, fine detail within the network of the outflow vasculature is lost when noise is suppressed (Figures 3 and 4). Commercially available systems can scan the limbus relatively quickly (Cirrus HD-OCT [Carl Zeiss Meditec], anterior segment 512 × 128-scan, 2-second acquisition time), providing visualization of the limbus for 3-D reconstructions of the outflow system. The lower scan density, however, produces less complete visualization of the aqueous outflow structures (Figure 5).

Future systems may compensate for these limitations. For example, the spectral signature of blood may be used to identify blood vessels within the scan. The absorption characteristics of hemoglobin may be used to discern blood from aqueous outflow vessels.[12] Furthermore, the automated identification of blood

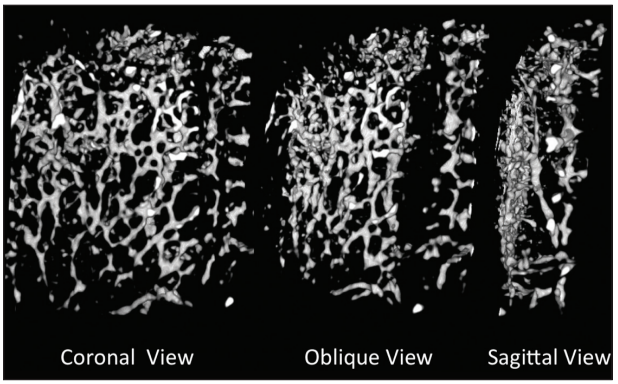

Figure 4. After the reduction of background clutter, the network of outflow vessels can be observed in 3-D space, visualizing the multilayered organization with connecting vessels between (right).

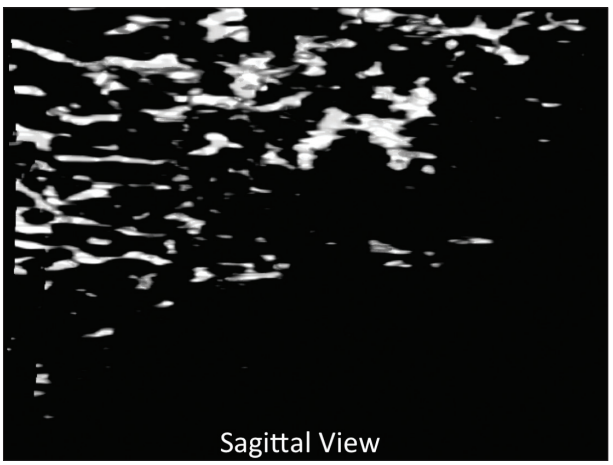

Figure 5. Unlike the experimental system sampling tissue with 512 × 512 A-scans, commercially available systems do not sample with sufficient A-scan density to create 3-D visualization of the same quality. Here, the outflow vasculature of a living eye was isolated from a typical 512 × 128 anterior segment scan using the Cirrus HD-OCT.

vessels' shadows, based on their characteristic vertical presentation, may allow localized enhancement in shadowed regions. This technique could recover image information and remove the shadow artifact that limits the application of connectivity requirements in the segmentation of the aqueous outflow vascular system.[13,14]

CONCLUSION

Work using cadaveric outflow models has provided pilot data demonstrating that the 3-D network of the outflow pathway can be discerned from the surrounding tissue. Clinically, this pathway can be subjectively followed by interrogating the image stack that makes up an OCT volumetric scan. To date, however, numerous sources of noise and competing vessels within the limbus region have thwarted attempts to automatically isolate and visualize the outflow pathway in living eyes. Advances in shadow suppression and the identification of blood within the spectral signature of OCT scan data may lead to a clinically viable automated solution to visualizing the outflow pathway in the near future. ■

Larry Kagemann, PhD, is an associate professor at the University of Pittsburgh School of Medicine in the Department of Ophthalmology, and he has a secondary academic appointment in the University of Pittsburgh Swanson School of Engineering in the Department of Bioengineering. He has no financial interest in the products or companies mentioned herein. Dr. Kagemann may be reached at (412) 648-6409; lek19@pitt.edu.

Joel S. Schuman, MD, is the distinguished Eye and Ear Foundation professor and chairman of the Department of Ophthalmology at the University of Pittsburgh School of Medicine, and he is the director of the UPMC Eye Center. He is also a professor of bioengineering at the University of Pittsburgh School of Engineering and a professor at the Center for the Neural Basis of Cognition, Carnegie Mellon University and University of Pittsburgh. Dr. Schuman receives royalties for intellectual property owned and licensed by Massachusetts Institute of Technology and Massachusetts Eye and Ear Infirmary to Carl Zeiss Meditec. Dr. Schuman may be reached at (412) 647-2205; schumanjs@upmc.edu.

1. Yi K, Mujat M, Park BH, et al. Spectral domain optical coherence tomography for quantitative evaluation of drusen and associated structural changes in non-neovascular age-related macular degeneration. *Br J Ophthalmol*. 2009;93(2):176-181.
2. Freeman SR, Kozak I, Cheng L, et al. Optical coherence tomography-raster scanning and manual segmentation in determining drusen volume in age-related macular degeneration. *Retina*. 2010;30(3):431-435.
3. Ko A, Cao S, Pakzad-Vaezi K, et al. Optical coherence tomography-based correlation between choroidal thickness and drusen load in dry age-related macular degeneration. *Retina*. 2013;33(5):1005-1010.
4. Nathoo NA, Or C, Young M, et al. Optical coherence tomography-based measurement of drusen load predicts development of advanced age-related macular degeneration [published online ahead of print June 28, 2014]. *Am J Ophthalmol*. doi:10.1016/j.ajo.2014.06.021.
5. Pachiyappan A, Das UN, Murthy TV, Tatavarti R. Automated diagnosis of diabetic retinopathy and glaucoma using fundus and OCT images. *Lipids Health Dis*. 2012;11:73.
6. Yang Q, Reisman CA, Chan K, et al. Automated segmentation of outer retinal layers in macular OCT images of patients with retinitis pigmentosa. *Biomed Opt Express*. 2011;2(9):2493-2503.
7. Kagemann L, Ishikawa H, Wollstein G, et al. Ultrahigh-resolution spectral domain optical coherence tomography imaging of the lamina cribrosa. *Ophthalmic Surg Lasers Imaging*. 2008;39(4 suppl):S126-131.
8. Wang B, Nevins JE, Nadler Z, et al. Reproducibility of in-vivo OCT measured three-dimensional human lamina cribrosa microarchitecture. *PloS One*. 2014;9(4):e95526.
9. Wang B, Nevins JE, Nadler Z, et al. In vivo lamina cribrosa micro-architecture in healthy and glaucomatous eyes as assessed by optical coherence tomography. *Invest Ophthalmol Vis Sci*. 2013;54(13):8270-8274.
10. Nadler Z, Wang B, Wollstein G, et al. Automated lamina cribrosa microstructural segmentation in optical coherence tomography scans of healthy and glaucomatous eyes. *Biomed Opt Express*. 2013;4(11):2596-2608.
11. Kagemann L, Wollstein G, Ishikawa H, et al. 3D visualization of aqueous humor outflow structures in-situ in humans. *Exp Eye Res*. 2011;93(3):308-315.
12. Kagemann L, Wollstein G, Wojtkowski M, et al. Spectral oximetry assessed with high-speed ultra-high-resolution optical coherence tomography. *J Biomed Opt*. 2007;12(4):041212.
13. Mari JM, Strouthidis NG, Park SC, Girard MJ. Enhancement of lamina cribrosa visibility in optical coherence tomography images using adaptive compensation. *Invest Ophthalmol Vis Sci*. 2013;54(3):2238-2247.
14. Girard MJ, Strouthidis NG, Ethier CR, Mari JM. Shadow removal and contrast enhancement in optical coherence tomography images of the human optic nerve head. *Invest Ophthalmol Vis Sci*. 2011;52(10):7738-7748.